Breakthrough studies with mono-, binary- and ternary-ion systems comprised of Fe(II), F^- and As(III) using river sand packed columns for groundwater treatment

Kamal Uddin Ahamad and Mohammad Jawed

ABSTRACT

Groundwater in Assam, India, contains excessive amounts of arsenic (As(III)), fluoride (F^-) and iron (Fe(II)). The rural and semi-urban population of Assam uses indigenous iron filters fabricated using processed sand (PS) as one of the chief constituents to reduce Fe(II) concentration; however, no efforts have been made to reduce As(III) or F^- concentrations before use. The present work is directed towards assessing the potential of PS for removal of these ions from mono-, binary- and ternary-ion systems through continuous mode column studies. Synthetic water samples containing fixed concentration of ions were prepared using deionized water. The observed order of breakthrough of ions was: As(III) followed by Fe(II) and F^- followed by Fe(II) in the case of the binary ion systems of Fe(II) + As(III) and Fe(II) + F^-. The throughput volume for As(III) in the (Fe(II) + As(III)) system and for F^- in the (Fe(II) + F^-) system is termed the critical breakthrough throughput volume. In the ternary ion system (Fe(II) + As(III) + F^-), the order of breakthrough of ions observed was F^-, then As(III) and then Fe(II) and hence the throughput volume F^- is termed the critical breakthrough throughput volume. Results of column studies also indicate the impact on the uptake of the selected ion by the presence of the other ion present in the binary- and ternary-ion systems.

Key words | adsorption, arsenic removal, breakthrough analysis, continuous column studies, iron removal

Kamal Uddin Ahamad (corresponding author)
Department of Civil Engineering,
Tezpur University,
Napaam, 784028,
Assam,
India
E-mail: *kahamad@tezu.ernet.in*

Mohammad Jawed
Department of Civil Engineering,
Indian Institute of Technology Guwahati,
Guwahati, 781039,
Assam,
India

INTRODUCTION

Groundwater is the major source of domestic water for people living in rural and semi-urban areas of Assam, a hilly northeastern province of India. The concentrations of arsenic (As(III)), fluoride (F^-) and iron (Fe(II)) in the groundwater have been reported to be in the range 0.05–0.2 mg/L, 5–23 mg/L and 1–25 mg/L, respectively (Das *et al.* 2003; Mahanta *et al.* 2004; Singh 2004; Sharma *et al.* 2005; Meenakshi & Maheshwari 2006); these values are much higher than the permissible limits in drinking water (0.01 mg/L for As(III), 1–1.5 mg/L for F^- and 0.3 mg/L for Fe(II))(IS 10500 1991; WHO 1993). The iron present in the groundwater causes visible coloration in the water and hence the rural and semi-urban population of Assam uses indigenous household iron filter units to reduce its concentration. The concentration of iron in the groundwater above regulatory limits makes the water unusable mainly from aesthetic considerations such as discoloration, metallic taste, odor, turbidity, staining of laundry and plumbing fixtures. Aeration and separation are the most common methods for removal of iron from groundwater in public water supply systems, but are not popular among rural and semi-urban communities lacking piped water supplies. Other methods available for iron removal from groundwater are ion-exchange (Vaaramaa & Lehto 2003), oxidation with oxidizing agents such as chlorine and potassium permanganate (Ellis *et al.* 2000), adsorption on activated carbon and other adsorbents (Munter *et al.* 2005) and treatment with limestone (Aziz *et al.* 2004). Intensive research has been

doi: 10.2166/wh.2013.157

undertaken in the last few decades in developing countries, including Sri Lanka, Ghana, Burkina Faso, Argentina, South Africa, Uganda and India, which has yielded many different methods, designs and configurations of iron removal units to be used at the community level (Chibi 1995; Andersson & Johansson 2002). But, surprisingly, none of the iron removal units so developed has found its place in rural and semi-urban areas, either at community level or at individual household level in this region, probably due to high capital costs and the complicated operation and maintenance requirements of these methods.

Since fluoride does not cause any visible coloration to water, no efforts are being made to reduce its concentration in groundwater before using it for drinking and cooking in rural and semi-urban areas of Assam. Defluoridation of drinking water is the only practicable option to overcome the problem of excessive fluoride in drinking water where alternate sources are not available. During the years following the discovery of fluoride as the cause of fluorosis, extensive research has been carried out on various methods for its removal from water (Larsen & Pearce 1992; Dahi 1996; Rajchagool & Rajchagool 1997; Venkobachar *et al.* 1997; Dzung *et al.* 2004; Ikuo *et al.* 2004).

Highlighting of the problems associated with the presence of arsenic in groundwater in Assam is just beginning. It has been reported that 20 out of 24 districts of Assam have groundwater with arsenic content exceeding 0.05 mg/L (Mahanta *et al.* 2004). Arsenic contamination in groundwater in developing countries poses a great threat to human health. The WHO drinking water guideline for arsenic was lowered from 0.05 to 0.01 mg/L in 1993 (WHO 1993) in consideration of epidemiological evidence of arsenic carcinogenicity. A number of household arsenic removal technologies have been developed or are still under development, including the two bucket treatment unit (Sarkar *et al.* 2000), Sono 3-Kolshi filter (Khan *et al.* 2000), well-head arsenic removal units (Sudipta *et al.* 2005), household sand filters (Berg *et al.* 2006), Kanchan arsenic filter (Ngai *et al.* 2007), BUET activated alumina arsenic removal unit (Garelick & Jones 2008), SAFI filter (Garelick & Jones 2008) and UNESCO-IHE arsenic removal family filter (Petrusevski *et al.* 2008). Some of these technologies have undergone field level trials with encouraging results. Household arsenic removal technologies are yet to find their place in the rural parts of Assam as a result of: (i) poor economic conditions of the rural population; (ii) non-availability of developed technologies; (iii) costly filtering media used and (iv) complex and tedious operation and maintenance to keep units functional. Since arsenic does not cause any visible coloration to groundwater, no efforts are made to reduce its concentration.

The rural population of Assam use variants of indigenous household iron filters to reduce excess concentration of iron (Fe(II)) in groundwater (Ahamad & Jawed 2010). These filters have been developed based on experiences of the rural population and passed on from previous generations. They have been fabricated using local materials such as community prepared wooden charcoal, sand and gravel (Ahamad & Jawed 2007). However, very limited scientific studies have been carried out to understand the role of the media used in these filters for removal of Fe(II) (Ahamad & Jawed 2010) and little effort has been made to improve their performance. Moreover when groundwater containing Fe(II), F^- and As(III) passes through these filters, the adsorption of the ions might be taking place from binary- ((Fe(II) + As(III)) or (Fe(II)+ F^-)) or ternary- ((Fe(II) + As(III) + F^-)) ion systems rather than mono-ion systems (Fe(II) or F^-or As(III) alone). Unfortunately, little literature is available dealing directly with removal of Fe(II) + As(III) or Fe(II)+ F^- + As(III) ions as part of binary- or ternary-ion systems from groundwater (Buamah 2009; Ahamad 2010). Therefore the objective of the present work is to assess the potential of processed sand (PS) for ion removal from synthetic water samples of mono-, binary- and ternary-ion systems comprised of Fe(II), F^- and As(III) through continuous mode column studies.

MATERIAL AND METHODS

River sand

River sand – a local construction material was procured from the village market (Amingaon) near the Indian Institute of Technology (IIT) Guwahati campus. The sand was mined from the river-beds where the Kulsi and Digaru rivers flow in to the Brahmaputra, approximately 50 and 35 km upstream, respectively, from the IIT Guwahati

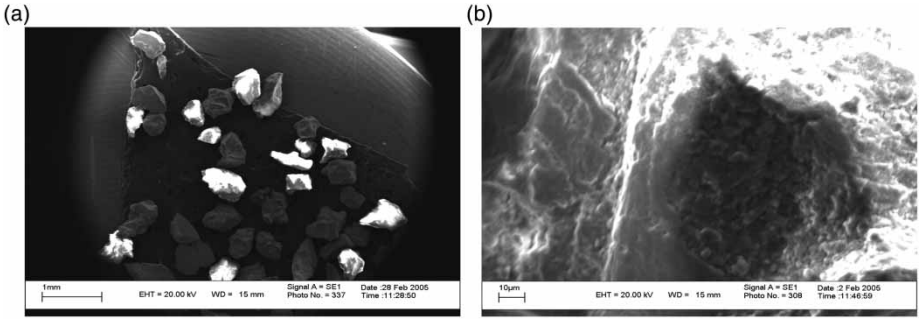

Figure 1 | Scanning electon micrographs of processed sand particles at magnification of (a) 1 mm, (b) 10 μm.

campus. The semi-urban and rural populations generally use this sand in indigenous household iron filter units. The river sand was washed with deionized water to remove foreign matter, such as floating debris, dirt and clay, dried at 105 °C in a hot air oven and then sieved (IS 2720 1975). Sand particles passing through 300 μm sieve openings but retained on 150 μm sieve openings were used for the study and termed PS. Scanning electron microscopy of PS (without interaction with dissolved iron, fluoride and arsenic) indicated the presence of undulating surfaces with crevices, as shown in Figure 1, whereas energy-dispersive X-ray spectroscopy indicated the presence of iron on the sand surface. The relevant properties of PS used for the study are presented in Table 1.

Stock mono-, binary- and ternary-ion solutions and other reagents

Stock solutions of Fe(II) (0.2 mg/mL), F^- (100 μg/mL) and As(III) (0.001 mg/mL) were prepared by dissolving the required amount of analytical grade $Fe(SO_4)_2.7H_2O$, As_2O_3 or NaF in deionized water. The initial pH of the stock solution was adjusted in the range 6.0–6.5 by addition of 0.1 N HNO_3 or NaOH solutions (Rao & Rekha 2004). The working solutions of binary- and ternary-ions were prepared by diluting stock solutions of mono-ions in deionized water. The initial concentrations were 5, 2 and 0.5 mg/L, respectively, for Fe(II), $F^-$and As(III) in mono-, binary- and ternary-ion systems. The residual concentrations of Fe(II) and As(III) were measured using an atomic absorption spectrophotometer (Model: 55 B, M/S Spectra AA Varian, Australia), and concentration of F^- was measured following the SPADNS method (APHA 1998) using a digital spectrophotometer (Model: 166, M/S Systronics India Ltd, India).

Table 1 | Characteristics of processed sand

Characteristic	Value
Particle size range (μm)	300–150
Bulk density (kg/m^3)	1,523
Moisture content (%)	0.5
Ash (Inert) content (%)	94
BET surface area (m^2/g)	0.28

BET: Brunauer-Emmett-Teller.

Continuous mode column studies

A series of continuous mode column studies were carried out to understand the effect of bed depths and the impact of linear flow rates on ion uptake by PS beds from mono-, binary- and ternary-ion systems comprised of Fe(II), F^- and As(III) using PVC columns of 3-cm internal diameter (Figure 2). Beds were compacted by putting PS in layers and imparting short jerks to the column in order to pack the bed to the required depth. A cotton plug (1 cm depth) was placed at the bottom of the bed to support the sand. Bed depths of 5, 10 and 15 cm in columns contained 57, 107 and 142 g of PS. The columns were operated continuously at room temperature (22 ± 1 °C) in down-flow mode using a peristaltic pump (Model: PA-SF, M/S IKA-WERKE, Germany) at constant linear flow rates of 1.5, 2.5 and 3.5 mL/min using the working solutions of Fe(II), F^- and As(III). These standard experimental conditions were used throughout the study. Samples from the column were collected at regular intervals until the bed was exhausted

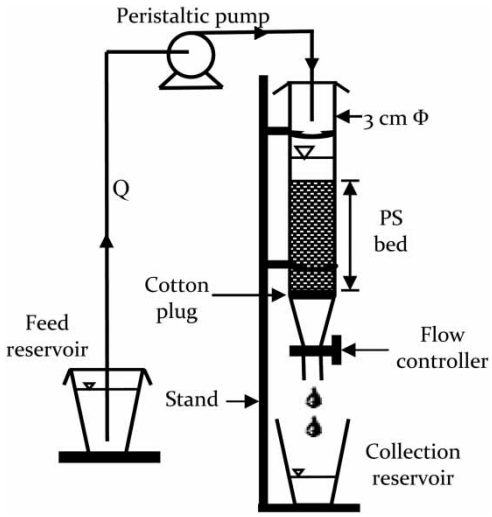

Figure 2 | Experimental set-up for continuous column studies.

or yielded effluent with 90% of initial ion concentrations. All column studies were carried out in duplicate.

RESULTS AND DISCUSSION

Breakthrough profiles of ion uptake by PS beds from mono-ion systems of Fe(II) alone, F⁻ alone and As(III) alone

The breakthrough curves for Fe(II), F⁻ and As(III) by PS bed depths of 5, 10 and 15 cm at three different linear flow rates of 1.5, 2.5 and 3.5 mL/min are presented in Figure 3, and the results in terms of breakthrough throughput volume (V_B) and corresponding service time (t_B) are summarized in

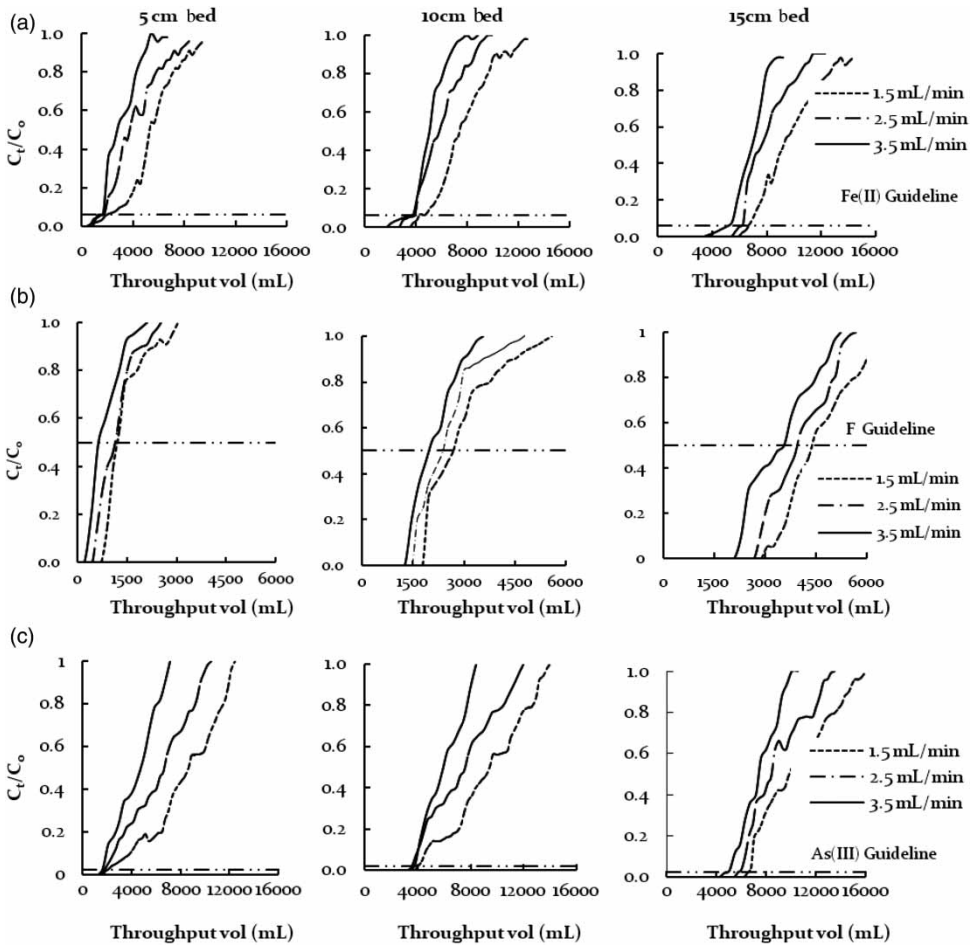

Figure 3 | Breakthrough curves for (a) Fe(II), (b) F⁻and (c) As(III) by PS bed depths of 5, 10 and 15 cm at flow rates of 1.5, 2.5 and 3.5 mL/min. Initial Fe(II) conc. = 5 mg/L, initial F⁻ conc. = 2 mg/L; initial As(III) conc. = 0.5 mg/L; initial pH = 5.5, temp. = 22 ± 1 °C. (Note: Only trend lines shown; individual data points have been removed to maintain the clarity of figures.)

Table 2. The V_B values were obtained when the mono-ion concentration in the effluent was less than or equal to the regulatory guidelines values, i.e. 0.3 mg/L for Fe(II), 1.0 mg/L for F^- and 0.01 mg/L for As(III) (WHO 1993). Similarly, the corresponding t_B values were also calculated for all V_B values obtained from the breakthrough curves. A decrease in V_B values was observed with increase in flow rates for the fixed bed depths (Table 2), indicating decreased amount of ion uptake by PS beds with increase in linear flow rates. The breakthrough curves showed a characteristic 'S' shaped profile produced in an ideal adsorption system. An increase in the linear flow rate reduced the volume treated until breakthrough point and therefore decreased the t_B of the bed. This was due to decrease in contact time between the ions and PS beds at higher linear flow rates. With increase in linear flow rates, the available time required to diffuse through the boundary layer might be less and therefore led to reduced V_B values.

In order to understand the effect of variation in PS bed depths on ion uptake from mono-ion systems, the data presented in Table 2 have been re-examined for V_B and t_B values by keeping the flow rate fixed but varying bed depths. The V_B values increased with increase in bed depths at the fixed flow rates. With increase in the bed depth, the mass transfer resulting from diffusion of ions increases while the mass transfer due to axial dispersion decreases. This appears to be in line with previous observations that when the bed depth was reduced, axial dispersion phenomena predominated in the mass transfer and reduced the diffusion of metallic ions (Costodes *et al.* 2005). An increase in the volume of solution treated was observed at the breakthrough point when the bed depth in the column increased from 5 to 15 cm. The increase in ion adsorption from the mono-ion system with increase in bed depth was a result of the increase in quantity of adsorbent mass in larger beds, which provided greater service area (or adsorption sites). The breakthrough time also increased with increase in depth of the bed.

Breakthrough profiles of ion uptake by PS beds from binary-ion systems comprised of (Fe(II) + As(III)) and (Fe(II) + F^-) ions

Breakthrough profiles of ion uptake by PS beds from binary-ion system comprised of Fe(II) and As(III) ions

Continuous column studies were carried out to observe ion uptake by PS beds from the binary-ion system of Fe(II) and As(III) using the standard experimental conditions. The breakthrough curves are presented in Figure 4 and results are summarized in Table 3. The order of breakthrough of ions present in the binary-ion system was: As(III) followed by Fe(II) for all bed depths and flow rates. At the breakthrough point of the selected ion, the concentration of the other ion in the effluent was also estimated and is presented in Table 3 against the V_B value of the selected ion. If the selected ion is Fe(II), its V_B value was 1,890 mL with 5 cm bed depth at a flow rate of 1.5 mL/min and the

Table 2 | Summary of breakthrough results with mono-ion system of Fe(II), F^- and As(III) operated at fixed bed depths of PS but with varying flow rates

		Fe(II) = 5 mg/L			F^- = 2 mg/L			As(III) = 0.5 mg/L		
Bed depth (cm)	Flow rate (mL/min)	V_B (mL)	t_B (min)	Amount adsorbed (mg)	V_B (mL)	t_B (min)	Amount adsorbed (mg)	V_B (mL)	t_B (min)	Amount adsorbed (mg)
5	1.5	1,970	1,313	9.25	1,440	960	1.44	1,730	1,153	0.848
	2.5	1,775	710	8.34	1,425	570	1.43	1,530	612	0.750
	3.5	1,520	434	7.14	1,165	332	1.17	1,250	357	0.613
10	1.5	4,250	2,833	19.98	2,700	1,800	2.70	3,975	2,650	1.948
	2.5	3,928	1,571	18.46	2,475	990	2.48	3,250	1,300	1.593
	3.5	3,875	1,107	18.21	2,100	600	2.10	3,350	957	1.642
15	1.5	6,670	4,446	31.35	4,340	2,893	4.34	6,250	4,166	3.063
	2.5	6,150	2,460	28.91	3,975	1,590	3.98	5,620	2,248	2.754
	3.5	5,270	1,505	24.77	3,425	978	3.43	4,670	1,134	2.288

V_B = Breakthrough throughput volumes at effluent mono-ion concentrations equal to regulatory limits; t_B = Service time at breakthrough.

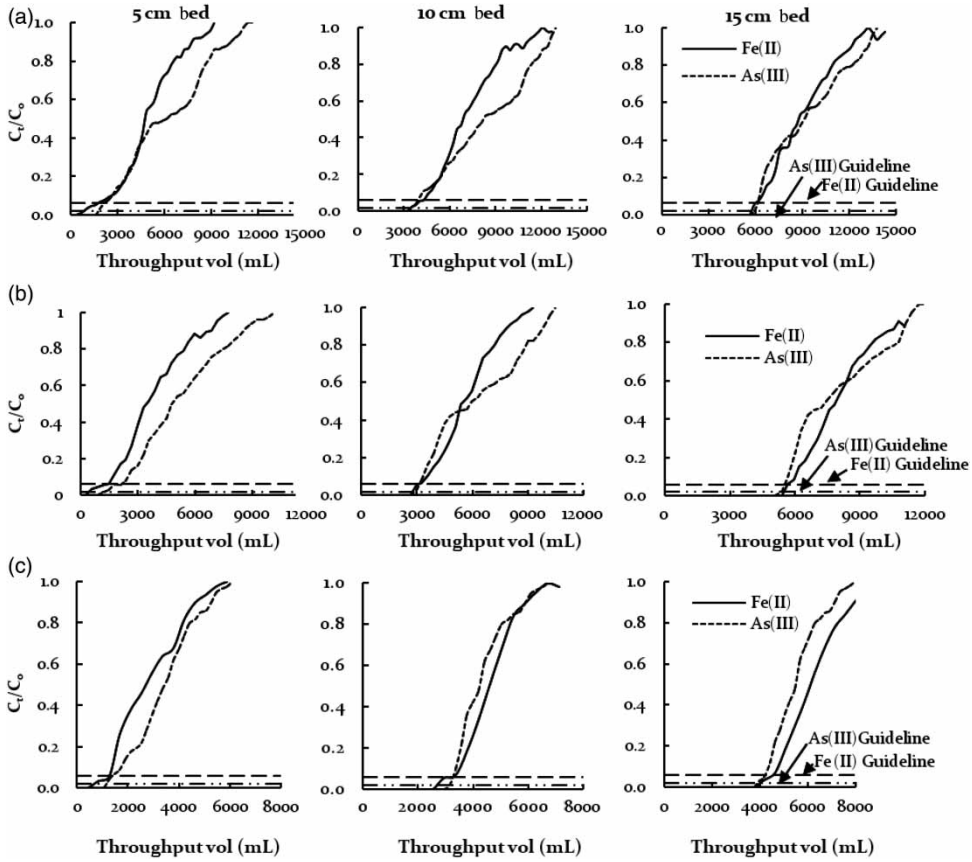

Figure 4 | Breakthrough curves for Fe(II) and As(III) from binary-ion system by PS bed depths of 5, 10 and 15 cm at a flow rate of (a) 1.5 mL/min (b) 2.5 mL/min and (c) 3.5 mL/min. Initial Fe (II) conc. = 5 mg/L, initial As(III) conc. = 0.5 mg/L; initial pH = 5.5, Temp = 22 ± 1 °C. (Note: Only trend lines shown while individual data points removed to maintain the clarity of figures.)

concentration of As(III), at the breakthrough point of Fe(II), was estimated as 0.015 mg/L. Similarly, if the selected ion is As(III), its V_B value was 1,700 mL with 5 cm bed depth at a flow rate of 1.5 mL/min and the concentration of Fe(II) was 0.26 mg/L at the breakthrough point of As(III). The results in Table 3 indicated that the concentration of Fe(II) in the effluent at breakthrough points of As(III) was less than 0.3 mg/L (IS 10500 1991) for all bed depths and flow rates. However, the concentrations of As(III) in the effluent at the breakthrough points of Fe(II) were greater than 0.01 mg/L (IS 10500 1991) for all bed depths and flow rates. It is clear that the V_B values obtained for As(III) for the binary-ion system appeared to be critical even if the other metal ion, i.e. Fe(II), was yet to break through. Therefore, in a binary-ion system, the ion breaking through first could play a critical role and the bed could be operated to produce the effluent satisfying the regulatory limits simultaneously in terms of both ions. Hence, for the Fe(II) and As(III) system, the V_B values obtained for As(III) for all bed depths and flow rates may be termed the critical breakthrough throughput volume (V_{BC}). The beds might be operated up to the V_{BC} values to obtain treated effluent meeting the regulatory guidelines limits simultaneously for both Fe(II) and As(III). However, it is important to note that the bed will be exhausted with respect to the ion having the critical breakthrough but still have potential to adsorb more of the other metal ion present in the binary-ion system if operated beyond the critical breakthrough point.

The amount of metal ion adsorbed by PS beds from the binary-ion system up to the V_{BC}s are shown in Table 4. For example, at V_{BC} = 1,700 mL for PS bed depth of 5 cm at a flow rate of 1.5 mL/min, the amount of metal ion adsorbed was 8.00 mg Fe(II) and 0.830 mg As(III) by 57 g of PS from the binary-ion system. The amount of metal ion adsorbed

Table 3 | Summary of breakthrough results of binary-ion system comprised of Fe(II) and As(III) operated at fixed flow rates but with varying PS bed depths

Flow rate (mL/min)	Bed depth (cm)	Ion	V_B (mL)	t_B (min)	Other ion conc. at V_B (mg/L)
1.5	5	Fe(II)	1,890	1,260	As(III) = 0.015
		As(III)	1,700	1,133	Fe(II) = 0.26
	10	Fe(II)	4,120	2,747	As(III) = 0.040
		As(III)	3,500	2,333	Fe(II) = 0.29
	15	Fe(II)	6,000	4,000	As(III) = 0.040
		As(III)	5,940	3,960	Fe(II) = 0.28
2.5	5	Fe(II)	1,500	600	As(III) = 0.015
		As(III)	1,200	480	Fe(II) = 0.28
	10	Fe(II)	3,300	1,320	As(III) = 0.025
		As(III)	2,800	1,120	Fe(II) = 0.26
	15	Fe(II)	5,670	2,268	As(III) = 0.030
		As(III)	5,400	2,160	Fe(II) = 0.26
3.5	5	Fe(II)	1,270	363	As(III) = 0.010
		As(III)	1,100	314	Fe(II) = 0.29
	10	Fe(II)	2,300	657	As(III) = 0.090
		As(III)	2,150	614	Fe(II) = 0.28
	15	Fe(II)	4,500	1,286	As(III) = 0.030
		As(III)	3,800	1,086	Fe(II) = 0.18

V_B = breakthrough throughput volumes at effluent metal conc. equal to regulatory limits; t_B = Service time at breakthrough.

Table 4 | Metal ions adsorbed by PS beds from binary-ion system until critical breakthrough points with respect to As(III)

			Metal ion adsorbed	
Flow rate (mL/min)	Bed depth (cm)	V_{BC} (mL)	Fe(II) (mg)	As(III) (mg)
1.5	5	1,700	8.00	0.830
	10	3,500	17.50	1.710
	15	5,920	28.40	2.900
2.5	5	1,200	5.60	0.580
	10	2,800	14.00	1.370
	15	5,400	24.80	2.650
3.5	5	1,100	5.20	0.540
	10	2,150	14.80	1.540
	15	3,800	19.00	1.860

was 9.26 mg Fe(II) and 0.848 mg As(III) from the individual mono-ion system (Table 2) up to the breakthrough points with two different PS beds of 5 cm depth (containing 57 + 57 = 114 g of PS) at a flow rate of 1.5 mL/min. These observations suggest that more metal ion is adsorbed from the mono-ion system than from the binary-ion system. If water from two different groundwater sources contained only mono-ion (either Fe(II) or As(III)), then such water should preferentially be treated by the mono-ion system to take advantage of higher metal ion adsorption capacity up to the breakthrough point of mono-metal ions. But a groundwater source containing binary-metal ions (such as Fe(II) and As(III)) needs to be treated by the binary-ion system up to the critical breakthrough point of the ion which breaks through first. The groundwater of Assam contains more than one metal ion and therefore, application of the binary-ion system appears to be the more appropriate choice.

In order to understand the impact of the other metal ion (i.e. As(III)) present in the binary-ion system on the breakthrough profile of the selected metal ion (i.e. Fe(II)), or vice-versa, the trend of the breakthrough profiles of the selected ion obtained from mono- and binary-ion systems are plotted in Figure 5 for Fe(II) and Figure 6 for As(III) for all bed depths and flow rates. The breakthrough trends of Fe(II) for all bed depths at 1.5 mL/min of flow rate (Figure 5(a)) yielded early breakthrough (i.e. left-ward shifting of trend lines) for Fe(II) from the binary-ion system even though the concentration of As(III) in this system was only 0.5 mg/L. Similar early breakthrough trends for Fe(II) and As(III) from the binary-ion system compared to equivalent mono-ion systems was observed for other flow rates and PS bed depths. The early breakthrough trends of the selected metal ion (i.e. Fe(II)) indicated impact of the other metal ion (i.e. As(III)) present in the system on the selected ion or vice-versa. The early breakthrough meant reduced V_B values as well as reduced uptake of the selected metal ion in the presence of the other metal ion in the binary-ion system compared to the mono-ion system. The V_B values and amount of metal ion adsorbed from both systems are summarized in Table 5. It clearly shows that the reduction in V_B values and amount of metal ion adsorbed from the binary-ion system compared to the mono-ion system.

Bed depth service time analysis for metal uptake by PS beds from binary-ion system comprised of Fe(II) and As (III) ions

A relationship to predict the performance of continuous adsorption columns based on a surface-interaction-rate theory (Bohart & Adams 1920) and used by other

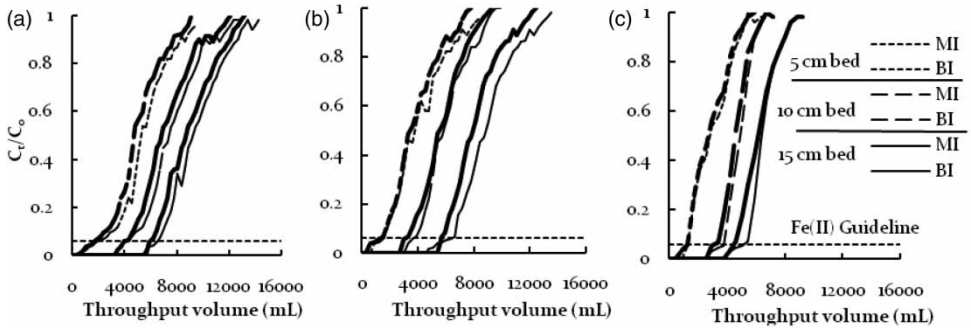

Figure 5 | Breakthrough trend of Fe(II) by PS bed depths of 5, 10 and 15 cm at flow rate of (a) 1.5 mL/min, (b) 2.5 mL/min and (c) 3.5 mL/min from mono- and binary-ion systems. Initial Fe(II) conc. = 5 mg/L, Initial As(III) conc. = 0.5 mg/L, Initial pH = 5.5, Temp. = 22 ± 1 °C. MI: mono-ion, BI: binary ion.

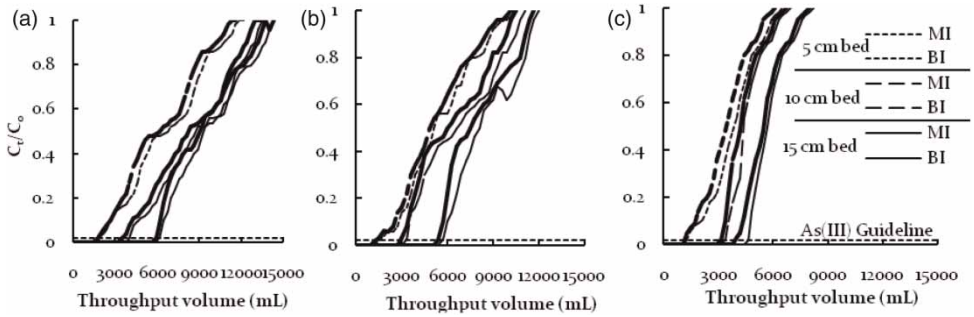

Figure 6 | Breakthrough trend of As(III) by PS bed depths of 5, 10 and 15 cm at flow rate of (a) 1.5 mL/min (b) 2.5 mL/min and (c) 3.5 mL/min from mono- and binary-metal ion systems. Initial Fe(II) conc. = 5 mg/L, Initial As(III) conc. = 0.5 mg/L, Initial pH = 5.5, Temp. = 22 ± 1 °C. MI: mono-ion, BI: binary ion.

Table 5 | Summary of breakthrough throughput volumes and amount of ions adsorbed by PS beds from mono- and binary-ion systems

		Mono-ion system				Binary-ion system			
		Fe(II)		As(III)		Fe(II)		As(III)	
Flow rate (mL/min)	Bed depth (cm)	V_B (mL)	Amount adsorbed (mg)	V_B (mL)	Amount adsorbed (mg)	V_B (mL)	Amount adsorbed (mg)	V_B (mL)	Amount adsorbed (mg)
1.5	5	2,350	11.04	1,950	0.956	2,230	10.48	1,620	0.793
	10	4,350	20.44	4,150	2.034	4,050	19.03	3,240	1.587
	15	6,950	32.66	6,520	3.195	6,790	31.91	5,940	2.910
2.5	5	2,100	9.87	1,720	0.843	2,080	9.77	1,500	0.735
	10	4,225	19.85	3,650	1.789	3,900	18.33	2,970	1.455
	15	6,425	30.19	5,970	2.925	6,300	29.61	5,500	2.695
3.5	5	1,820	8.55	1,490	0.730	1,700	7.99	980	0.480
	10	4,025	18.91	3,750	1.838	3,800	17.86	2,500	1.225
	15	5,670	26.64	4,950	2.426	5,200	24.44	4,190	2.053

researchers (Othman *et al.* 2001; Goel *et al.* 2005) is represented as:

$$\ln\left(\frac{C_o}{C_B}-1\right)=\ln\left(e^{KN_ox/v}-1\right)-KC_ot \quad (1)$$

where t is the service time, v is the linear flow rate, x is the depth of bed, K is the rate constant, N_o is the adsorptive capacity, C_o is the influent metal concentration and C_B is the allowable effluent metal concentration. Since $e^{KN_ox/v} >> 1$, Equation (1) is simplified to have a linear relationship between depth (x) and service time (t) (Muraleedharan *et al.* 1994; Lehman *et al.* 2001) as:

$$t=\frac{N_o}{C_ov}\left[x-\frac{v}{KN_o}\ln\left(\frac{C_o}{C_B}-1\right)\right] \quad (2)$$

The adsorptive capacity N_o could be determined from the slope of the linear plot of t versus x. The rate constant K is then calculated from the intercept of the linear plot. The intercept and the slope could be represented as:

$$\text{slope}=\frac{N_o}{C_ov} \quad (3)$$

$$\text{intercept}=-\frac{1}{KC_o}\ln\left(\frac{C_o}{C_B}-1\right) \quad (4)$$

The major limitation of this approach is that it requires at least nine individual column tests to collect the laboratory data required for design – an expensive and time-consuming proposition. An alternative technique – bed depth service time (BDST) (Hutchins 1973) requires only three column tests to collect the necessary data for the design and Equation (2) is expressed as:

$$t=ax+b \quad (5)$$

where a = slope (see Equation (3)) and b = intercept (see Equation (4)). According to the BDST approach, if the value of a is determined for one flow rate, values for other flow rates (a') could be calculated by multiplying the original slope a by the ratio of the original (F) and new flow (F') rates (Ahamad & Jawed 2010):

$$a'=a\,(F/F') \quad (6)$$

It is not necessary to adjust the b value, since this term is assumed to be insignificantly affected by change in the flow rates. In the case of the Fe(II) and As(III) binary-ion system, the V_B values obtained for As(III) by all bed depths and flow rates were termed V_{BC} because the effluent produced satisfied regulatory guideline limits for both metal ions in the binary-ion system. Therefore, BDST analysis was carried out only for As(III) metal ion which yielded critical breakthrough throughput from the binary-ion system. The estimated BDST parameters (N_o and K) for adsorption of As(III) from the binary-ion systems are presented in Table 6. The experimental BDST curves for As(III) adsorption from these systems were developed by plotting service times obtained at the critical breakthrough points with the three bed depths are shown in Figure 7. From the experimental BDST curve obtained for a particular flow rate through the bed, efforts were made to model BDST curves for the other two flow rates using Equations (5) and (6) and the modeled BDST curves were termed 'predicted BDST curves'. The experimental BDST curve obtained for As(III) adsorption at a flow rate of 1.5 mL/min by PS beds was used to develop the predicted BDST curves for the other two flow rates as shown in Figure 7. Similar modeling was also carried out for As(III) adsorption by selecting the experimental BDST curve of another flow rate and predicting BDST curves for the other two flow rates. However, the predicted BDST curves have not been shown. Instead, errors involved in predicted and experimental BDST curves obtained for the other two flow rates while using the experimental BDST curve of a particular flow rate

Table 6 | Estimated BDST parameters for As(III) adsorption by PS beds from binary-ion system

Ion (Initial conc.)	Flow rate (mL/min)	N_o (kg/m^3)	K (m^3/kg-min)	R^2
Fe(II) (5 mg/L) + As(III) (0.5 mg/L)	1.5	0.030	22.744	0.9929
	2.5	0.028	24.323	0.9709
	3.5	0.019	77.836	0.9838

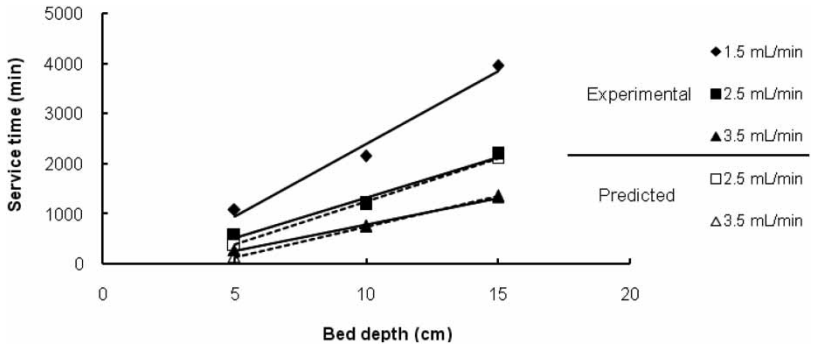

Figure 7 | Experimental and predicted BDST curves for As(III) adsorption by PS beds from the binary-ion system. Experimental BDST curve at flow rate of 1.5 mL/min with initial Fe(II) conc. = 5 mg/L and initial As(III) conc. = 0.5 mg/L used for prediction.

Table 7 | Estimated errors involved between predicted and experimental BDST values for As(III) adsorption from the binary-ion system

Ion (Initial conc.)	Selected flow rate (mL/min)	Predicted flow rate (mL/min)	Error (%) involved in service times for bed depth of		
			5 cm	10 cm	15 cm
Fe(II) (5 mg/L) + As(III) (0.5 mg/L)	1.5	2.5	4.85	19.78	0.97
		3.5	15.78	8.85	7.52
	2.5	1.5	9.85	0.85	6.98
		3.5	19.85	16.85	9.85
	3.5	1.5	12.68	2.96	0.75
		2.5	7.68	12.85	10.85

were estimated and tabulated in Table 7. The minimum and maximum errors involved between predicted and experimental BDST curves of As(III) adsorption varied between 0.85 and 19.86%.

Breakthrough profiles of ion uptake by PS beds from binary-ion system comprising Fe(II) and F⁻ ions

Continuous column studies were carried out to observe ion uptake from the Fe(II) and F⁻ binary-ion system. The breakthrough curves are presented in Figure 8 and results are summarized in Table 8. The order of breakthrough of ions was F⁻ followed by Fe(II) for all bed depths and flow rates. At the breakthrough point of the selected ion (i.e. Fe(II)), the concentration of the other ion (i.e. F⁻) in the effluent was also estimated and is presented in Table 8 against the V_B value of Fe(II), or vice-versa. If the selected ion is Fe(II), the V_B value for Fe(II) obtained with 5 cm bed depth at a flow rate of 1.5 mL/min was 1,890 mL while the concentration of F⁻ at the breakthrough point of Fe(II) was estimated as 1.8 mg/L. Similarly, if the selected ion is F⁻, the V_B value for F⁻ obtained with 5 cm bed depth at a flow rate of 1.5 mL/min was 1,350 mL while Fe(II) was detected at 0.08 mg/L at the F⁻ breakthrough point. The results in Table 8 indicated that the concentration of Fe(II) in the effluent F⁻ breakthrough points was less than 0.3 mg/L (i.e. the regulatory limit; IS 10500 1991) for all bed depths and flow rates. However, the concentration of F⁻ in the effluent at the Fe(II) breakthrough point was greater than 1 mg/L (i.e. the regulatory limit; IS 10500 1991) for all bed depths and flow rates. It is clear that the V_B values obtained for F⁻ for the binary-ion system with PS beds appeared to be critical even if the Fe(II) was yet to break through through the beds. Hence, in the case of the binary-ion system of Fe(II) and F⁻, the V_B values obtained for F⁻ for all bed depths and different flow rates may be termed the V_{BC}. The beds might be operated up to the V_{BC} values to obtain treated effluent meeting the regulatory guidelines limits simultaneously for both Fe(II) and F⁻.

The amount of ion adsorbed from the binary-ion system up to V_{BC}s are shown in Table 9. For example, at V_{BC} = 1,350 mL for PS bed depth of 5 cm at a flow rate of 1.5 mL/min, the amounts of ion adsorbed were 6.51 mg of Fe(II) and 1.35 mg of F⁻ by 57 g of PS. By comparison, the amounts of ion adsorbed from the individual mono-ion systems (Table 2) were 9.25 mg of Fe(II) and 1.44 mg of F⁻ until the breakthrough points with two different PS beds of 5 cm depth (containing 57 + 57 = 114 g of PS) at a flow rate of 1.5 mL/min. As for the Fe(II) + As(III), discussed

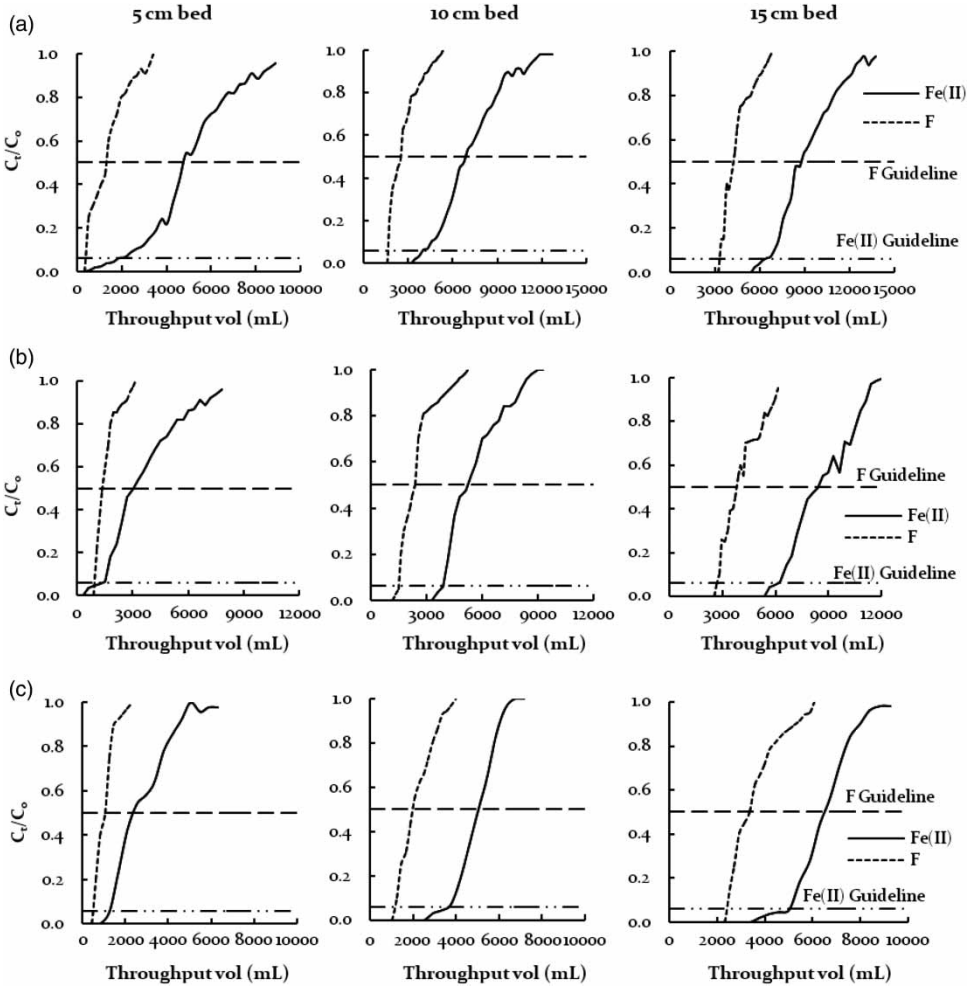

Figure 8 | Breakthrough curves for Fe(II) and F^- from binary-ion system by PS bed depths of 5, 10 and 15 cm at a flow rate of (a) 1.5 mL/min (b) 2.5 mL/min and (c) 3.5 mL/min. Initial Fe(II) conc. = 5 mg/L, initial F^- conc. = 2 mg/L; initial pH = 5.5, Temp. = 22 ± 1 °C. (Note: Only trend lines shown; individual data points removed to maintain the clarity of figures.)

above, these observations apparently suggest that more ions are adsorbed from the mono-ion system than from the binary-ion system, and reinforces the idea that groundwater containing mono-ions should be treated by the mono-ion system. But for a groundwater source containing binary-ions (such as Fe(II) and F^-) needs to be treated by the binary-ion system up to the critical breakthrough point of the ion which is breaking through first.

In order to understand the impact of the other ion (i.e. F^-) present in the binary-ion system on the breakthrough profile of the selected ion (i.e. Fe(II)) or vice-versa, the trend of breakthrough profile of the selected ion obtained from the mono- and binary-ion systems are plotted in Figure 9 for Fe(II) and Figure 10 for F^-. The breakthrough trends of Fe(II) for all PS bed depths at 1.5 mL/min of flow rate (Figure 9(a)) yielded early breakthrough (i.e. left-ward shifting of trend lines) for Fe(II) from the binary-ion system even though the concentration of F^- in this system was only 2 mg/L. Similar early breakthrough trends for Fe(II) and F^- from the binary-ion system was observed for other flow rates and PS bed depths. This early breakthrough indicated the impact of the other ion present in the system on the selected ion. The early breakthrough meant reduced V_B values as well as reduced uptake of the selected ion in the presence of the other ion present in the binary-ion system compared to the mono-ion system. The V_B values and amount of ion adsorbed from Fe(II) and F^- ion systems

Table 8 | Summary of breakthrough results with binary-ion system comprising Fe(II) and F⁻ operated at fixed flow rates but with varying bed depths of PS

Flow rate (mL/min)	Bed depth (cm)	Ion	V_B (mL)	t_B (min)	Other ion conc. at V_B (mg/L)
1.5	5	Fe(II)	1,890	1,260	$F^- = 1.8$
		F^-	1,350	900	Fe(II) = 0.08
	10	Fe(II)	3,970	2,647	$F^- = 1.8$
		F^-	2,670	1,780	Fe(II) = 0
	15	Fe(II)	6,520	4,347	$F^- = 2$
		F^-	4,220	2,813	Fe(II) = 0
2.5	5	Fe(II)	1,690	676	$F^- = 1.7$
		F^-	1,200	480	Fe(II) = 0.2
	10	Fe(II)	3,820	1,528	$F^- = 1.8$
		F^-	2,400	960	Fe(II) = 0
	15	Fe(II)	5,970	2,388	$F^- = 2$
		F^-	3,850	1,540	Fe(II) = 0
3.5	5	Fe(II)	1,480	423	$F^- = 1.8$
		F^-	1,050	300	Fe(II) = 0
	10	Fe(II)	3,800	1,086	$F^- = 1.5$
		F^-	2,030	580	Fe(II) = 0
	15	Fe(II)	5,180	1,480	$F^- = 1.9$
		F^-	3,360	960	Fe(II) = 0

V_B = Breakthrough throughput volumes at effluent metal conc. equal to regulatory limits (IS 10500 1991); t_B = Service time at breakthrough.

Table 9 | Ions adsorbed by PS beds from the binary-ion system until critical breakthrough points with respect to F⁻

			Ion adsorbed	
Flow rate (mL/min)	Bed depth (cm)	V_{BC} (mL)	Fe(II) (mg)	F^- (mg)
1.5	5	1,350	6.51	1.35
	10	2,670	13.35	2.67
	15	4,220	21.10	4.22
2.5	5	1,200	5.64	1.20
	10	2,400	12.00	2.40
	15	3,850	19.25	3.85
3.5	5	1,050	5.25	1.05
	10	2,030	10.15	2.03
	15	3,360	16.80	3.36

are summarized in Table 10. It clearly shows the reduction in V_B values, as well as amount of ions adsorbed from the binary-ion system compared to mono-ion system.

Bed depth service time analysis for ion uptake by PS beds from binary-ion system comprised of Fe(II) and F⁻ ions

In the case of the Fe(II) and F⁻ binary-ion system, the V_B values obtained for F⁻ for all bed depths and flow rates were termed the V_{BC} because the treated effluent satisfied regulatory guideline limits simultaneously for both ions present in the binary-ion system. Therefore, BDST analysis was carried out only for the F⁻ ion which yielded critical breakthrough throughput from the binary-ion system. The estimated BDST parameters (N_o and K) for adsorption of F⁻ from the binary-ion system are presented in Table 11. The experimental BDST curves for F⁻ adsorption from the binary-ion system were developed by plotting service times obtained at the critical breakthrough points with the respective bed depths (Figure 11). From the experimental BDST curve obtained for a particular flow rate through the bed, efforts were made to model BDST curves for other two flow rates using Equations (5) and (6) and the modeled BDST curves were termed predicted BDST curves. The experimental BDST curve obtained for F⁻ adsorption at a flow rate of 1.5 mL/min by PS beds were used to develop the predicted BDST curves for the other two flow rates (Figure 11). Similar modeling was also carried out for F⁻ adsorption by selecting the experimental BDST curve of another flow rate and predicting BDST curves for the remaining two flow rates. Errors involved in predicted and experimental BDST curves obtained for other two

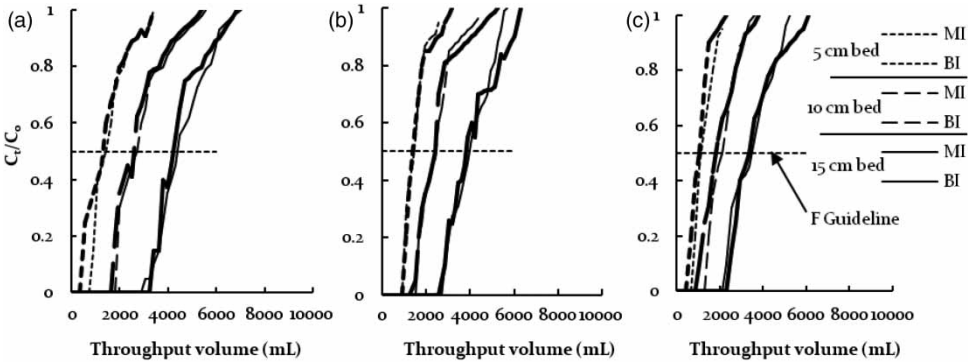

Figure 9 | Breakthrough trend of Fe(II) by PS bed depths of 5, 10 and 15 cm at flow rate of (a) 1.5 mL/min (b) 2.5 mL/min and (c) 3.5 mL/min from mono- and binary-ion systems. Initial Fe(II) conc. = 5 mg/L, initial F^- conc. = 2 mg/L; initial pH = 5.5, temp. = 22 ± 1 °C. MI: mono-ion, I: binary-ion.

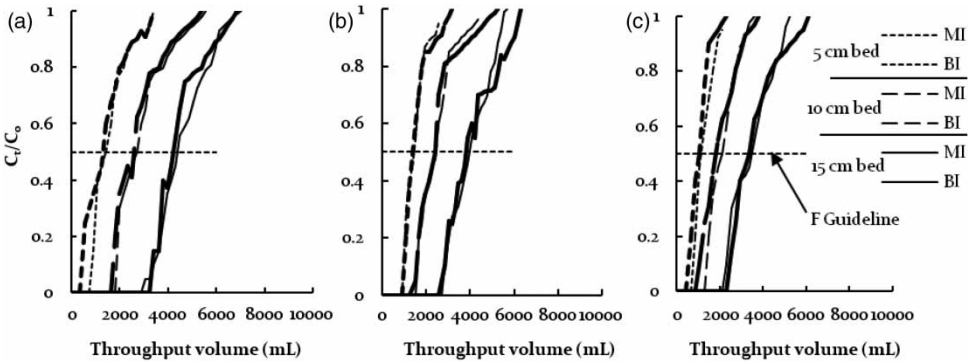

Figure 10 | Breakthrough trend of F^- by PS bed depths of 5, 10 and 15 cm at flow rate of (a) 1.5 mL/min (b) 2.5 mL/min and (c) 3.5 mL/min from mono- and binary-ion systems. Initial Fe(II) conc. = 5 mg/L, initial F^- conc. = 2 mg/L; initial pH = 5.5, temp. = 22 ± 1 °C. MI: mono-ion, I: binary-ion.

Table 10 | Summary of breakthrough throughput volumes and amount of ions adsorbed by PS beds from mono- and binary-ion systems

		Mono-ion system				Binary-ion system			
		Fe(II)		F^-		Fe(II)		F^-	
Flow rate (mL/min)	Bed depth (cm)	V_B (mL)	Amount adsorbed (mg)	V_B (mL)	Amount adsorbed (mg)	V_B (mL)	Amount adsorbed (mg)	V_B (mL)	Amount adsorbed (mg)
1.5	5	1,970	9.25	1,440	1.44	1,890	8.88	1,350	1.35
	10	4,250	19.97	2,700	2.70	3,970	18.65	2,670	2.67
	15	6,670	31.34	4,340	4.34	6,520	30.64	4,220	4.22
2.5	5	1,775	8.34	1,425	1.43	1,690	7.94	1,200	1.20
	10	3,928	18.46	2,475	2.48	3,820	17.95	2,400	2.40
	15	6,150	28.90	3,975	3.98	5,970	28.05	3,850	3.85
3.5	5	1,520	7.14	1,165	1.17	1,480	6.95	1,050	1.05
	10	3,875	18.21	2,100	2.10	3,800	17.86	2,030	2.03
	15	5,270	24.76	3,425	3.43	5,180	24.34	3,360	3.36

Table 11 | Estimated BDST parameters for F^- adsorption by PS beds from binary-ion system comprised of Fe(II) and F^-

Ion (Initial conc.)	Flow rate (mL/min)	N_o (kg/m^3)	K (m^3/kg-min)	R^2
Fe(II) (5 mg/L) + F^- (2 mg/L)	1.5	0.081	1.220	0.9979
	2.5	0.075	1.505	0.9970
	3.5	0.065	2.149	0.9924

flow rates while using the experimental BDST curve of a particular flow rate were estimated and are shown in Table 12. The minimum and maximum errors involved between predicted and experimental BDST curves of F^- adsorption varied between 0.97 and 21.11%.

Continuous mode column studies for ion uptake by PS beds from ternary-ion systems

The groundwater of Assam contains not only Fe(II) ions but also F^- and As(III) ions and hence further continuous mode column studies were carried out using the ternary-ion system comprised of Fe(II) + F^- + As(III) to observe the impact on breakthrough profiles as well as ion adsorption by PS beds. The PS bed depths and flow rates were the same as in previous experiments. The initial concentrations of ions in the ternary-ion systems were: Fe(II) = 5 mg/L, F^- = 2 mg/L and As(III) = 0.5 mg/L.

Breakthrough profiles of ion uptake by PS beds from a ternary-ion system comprised of Fe(II), F^- and As(III) ions

The breakthrough curves for ion adsorption from the Fe(II), F^- and As(III) ternary-ion system are presented in Figure 12. The order of breakthrough of ions was F^- followed by As(III) and then Fe(II) for all PS bed depths and flow rates. The breakthrough analysis indicated that concentrations of Fe(II) and As(III) in the effluents at points of breakthrough of F^- were less than 0.3 and 0.01 mg/L, respectively (i.e. the regulatory limit) for all bed depths and flow rates. However, the concentrations of either Fe(II) and F^- or F^- and As(III) in the effluent at the point of breakthrough of As(III) or Fe(II) were more than the regulatory limits (IS 10500 1991) in all cases. It is clear that the breakthrough throughput volumes obtained for F^- by PS beds from the ternary-ion appeared to be critical even if the other two ions were yet to break through through the beds. Therefore, in a ternary-ion system, the ion yielding breakthrough first through the bed could play a critical role and the bed could be operated to produce the effluent satisfying the regulatory limits simultaneously in terms of all the three ions. Hence, for the Fe(II), F^- and As(III) ternary-ion system; the breakthrough throughput volumes obtained for F^- for all bed depths and flow rates may be termed the critical breakthrough throughput volume (V_{BC}). The PS beds might be operated up to the critical breakthrough throughput volumes to obtain treated effluent meeting the regulatory guidelines limits simultaneously for all the three ions present in the ternary-ion system (i.e. 0.3 mg/L for Fe(II), 1.0 mg/L for F^- and 0.01 mg/L for As(III); IS 10500 1991). However, it is important to note that the bed will be exhausted in respect of the ion having critical breakthrough, but have potential to adsorb more of the other ions present in the system if operated beyond the critical breakthrough points.

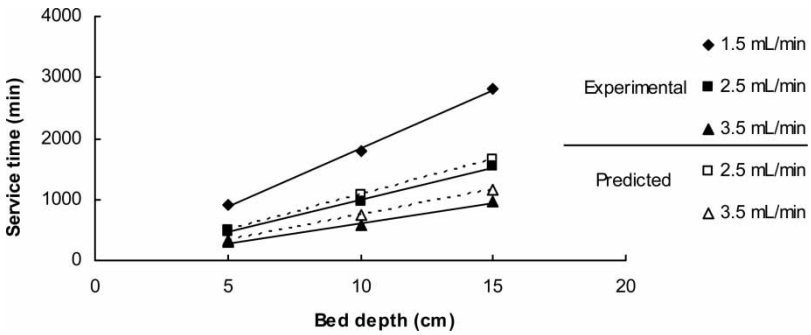

Figure 11 | Experimental and predicted BDST curves for F^- adsorption by PS beds at flow rates of 2.5 and 3.5 mL/min from binary-ion system comprised of Fe(II) and F^-. Experimental BDST curve at flow rate of 1.5 mL/min with initial Fe(II) conc. = 5 mg/L and initial F^- conc. = 2 mg/L used for prediction.

Table 12 | Estimated errors involved between predicted and experimental BDST values for F⁻ adsorption by PS beds from binary-ion system comprised of Fe(II) and F⁻

Ion (Initial conc.)	Selected flow rate (mL/min)	Predicted flow rate (mL/min)	Error (%) involved in service times for bed depth of 5 cm	10 cm	15 cm
Fe(II) (5 mg/L) + F⁻ (2 mg/L)	1.5	2.5	2.97	10.97	6.95
		3.5	8.87	26.98	19.85
	2.5	1.5	8.95	4.12	7.96
		3.5	21.11	18.95	6.85
	3.5	1.5	19.77	15.75	19.87
		2.5	0.97	14.88	5.95

In order to understand the impact of other two ions, i.e. F⁻ and As(III) or Fe(II) and As(III) or Fe(II) and F⁻, in the ternary-ion system on the breakthrough profile of the selected metal ion, i.e. Fe(II) or F⁻ or As(III), the trend of breakthrough profile of the selected ions from the binary- and ternary-ion systems are re-plotted in Figures 13–15. Figure 13 clearly indicates left-ward shifting of breakthrough trends obtained for Fe(II) with the ternary-ion system compared to the binary-ion system. Similar left-ward shifting of breakthrough trends for F⁻ and As(III) were observed for all flow rates and bed depths. Ideally, the trends of breakthrough profile obtained with mono-ion systems should have been included in these plots, but this might have compromised the clarity of these figures. However, left-ward shifting of trends of breakthrough profiles of binary-ion systems compared to mono-ion system were also observed, and hence it could be deduced that the trends of breakthrough profiles obtained with mono-ion systems will occupy extreme right positions while the trends of breakthrough profiles obtained with ternary-ion system occupy the extreme left positions, and the trends of breakthrough profiles obtained with binary-ion systems occupy intermediate positions. The left-ward shifting of breakthrough trends of metal ion indicated the impact of the other two metal ions present in the ternary-ion system on the selected ion compared to binary-ion systems. This left-ward shift meant reduced breakthrough throughput volumes as well as reduced amount of ion adsorbed by PS beds in the presence of the other two ions present in the ternary-ion system compared to binary-ion systems. The breakthrough throughput volumes and amount of ion adsorbed obtained with ternary-metal ion system is presented in Table 13. A reduction in breakthrough throughput volumes as well as amount of ion adsorbed from the ternary-ion system was observed when compared with corresponding binary-ion system (Table 5 for Fe(II) + As(III) and Table 10 for Fe(II) + F⁻).

The amounts of ion adsorbed by PS beds from the ternary-ion system up to the critical breakthrough throughput volumes (V_{BC}) are shown in Table 14. For example, at $V_{BC} = 1{,}350$ mL for PS bed depth of 5 cm at a flow rate of 1.5 mL/min, the amounts of ion adsorbed were 6.51 mg of Fe(II), 0.65 mg of F⁻ and 1.350 mg of As(III) by 57 g of PS. By comparison, the amounts of ion adsorbed were 9.26 mg of Fe(II), 1.44 mg of F⁻ and 0.848 mg of As(III) from the mono-ion system (Table 2) up to the breakthrough points with three different PS beds of 5 cm depth (having 57 g of PS in each bed) at a flow rate of 1.5 mL/min. These observations suggest higher metal adsorption by the mono-ion system than the ternary-ion system. If water from three different groundwater sources contained only mono-ions (either Fe(II) or F⁻ or As(III)), such water should be treated by the mono-ion system to take advantage of higher adsorption up to the breakthrough point of mono-ions. But a groundwater containing ternary-ion (such as Fe(II), F⁻ and As(III)) needs to be treated by the ternary-ion system up to the critical breakthrough point of the ion which is breaking through first. The groundwater of Assam contains more than one metal ion and therefore, application of ternary-metal ion system appears to be the most appropriate choice if treated only with PS beds for the removal of Fe(II), F⁻ and As(III) simultaneously.

Bed depth service time analysis for ion uptake by PS beds from ternary-ion system comprised of Fe(II), F⁻ and As(III) ions

For the Fe(II), F⁻ and As(III) ternary-ion system, the breakthrough throughput volumes obtained for F⁻ for all bed depths were termed the critical breakthrough throughput volume (V_{BC}) because it produced treated effluent satisfying regulatory guidelines limits simultaneously for the three ions. Therefore, BDST analysis was carried out only for F⁻

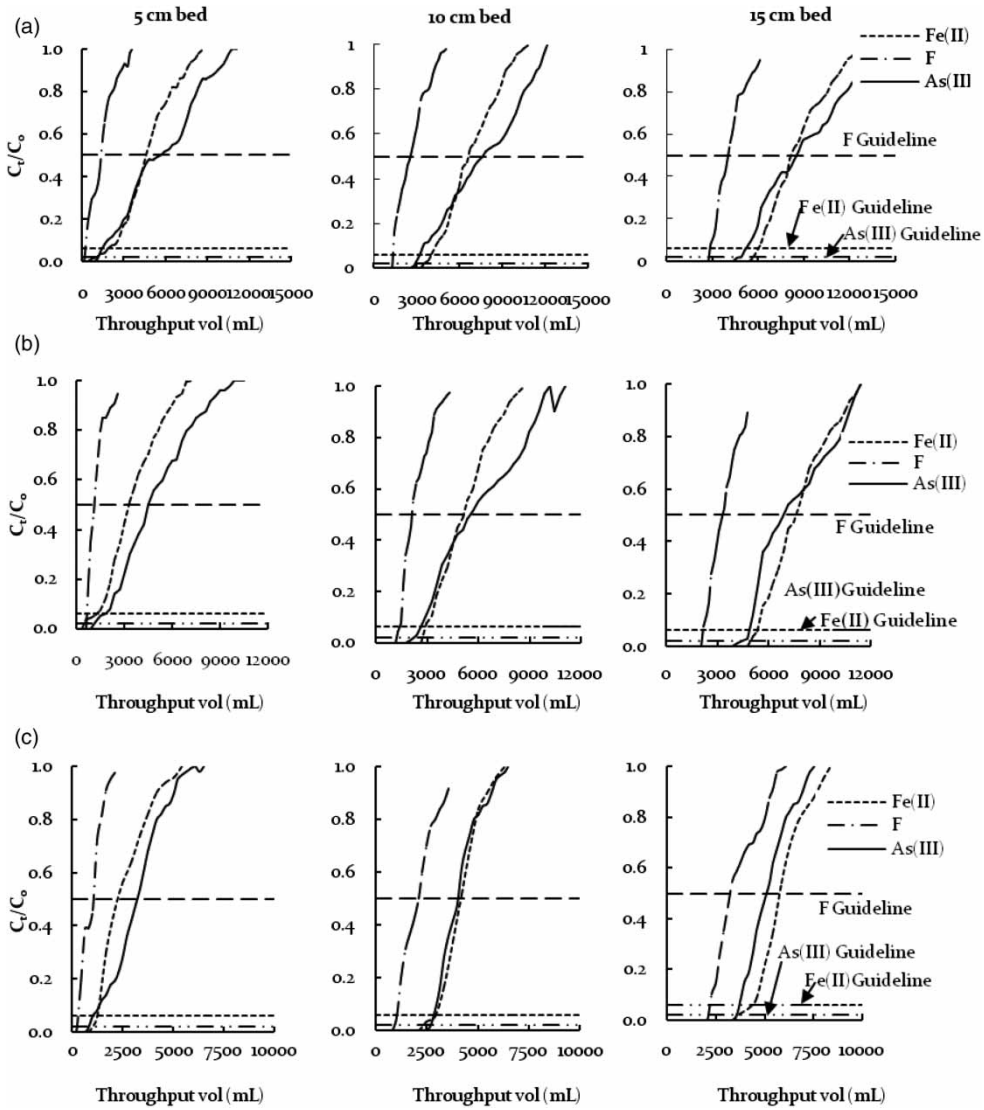

Figure 12 | Breakthrough curves for Fe(II), F⁻ and As(III) adsorption by PS bed depths of 5, 10 and 15 cm at a flow rate of (a) 1.5 mL/min, (b) 2.5 mL/min and (c) 3.5 mL/min from ternary-ion system comprised of Fe(II), F⁻ and As(III). Initial Fe(II) conc. = 5 mg/L, initial F⁻ conc. = 2 mg/L, initial As(III) conc. = 0.5 mg/L; initial pH = 5.5, temp. = 22 ± 1 °C.

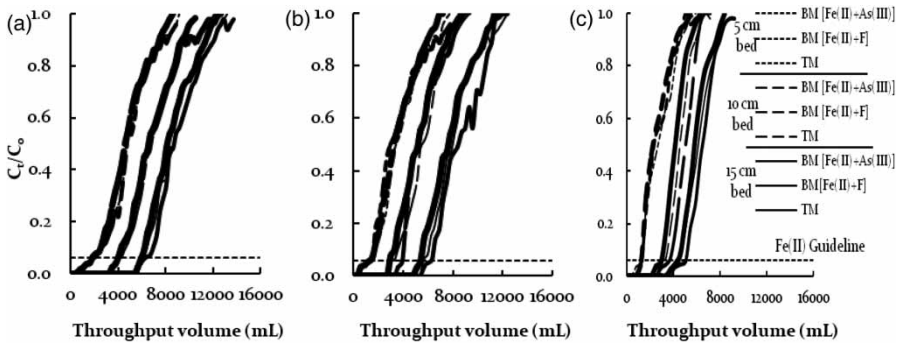

Figure 13 | Breakthrough trend of Fe(II) adsorption by PS bed depths of 5, 10 and 15 cm at flow rate of (a) 1.5 mL/min (b) 2.5 mL/min and (c) 3.5 mL/min from binary- and ternary-ion systems. Initial Fe(II) conc. = 5 mg/L, initial F⁻ conc. = 2 mg/L, initial As(III) conc. = 0.5 mg/L; initial pH = 5.5, temp. = 22 ± 1 °C. MI: mono-ion, I: binary-ion.

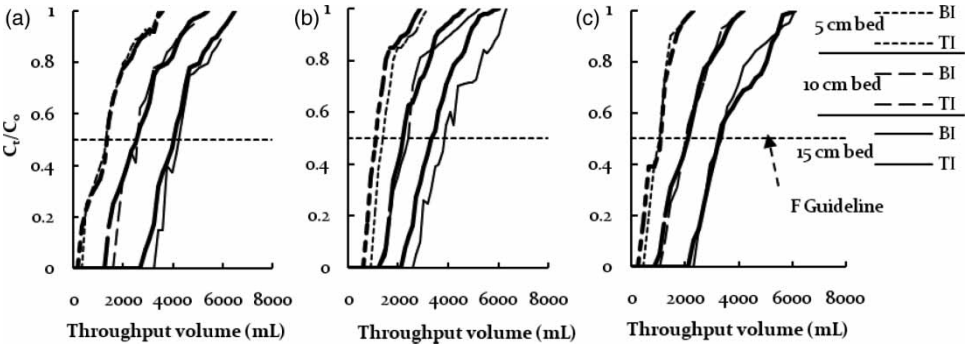

Figure 14 | Breakthrough trend of F^- adsorption by PS bed depths of 5, 10 and 15 cm at flow rate of (a) 1.5 mL/min (b) 2.5 mL/min and (c) 3.5 mL/min from binary- and ternary-metal ion systems. Initial Fe(II) conc. = 5 mg/L, initial F^- conc. = 2 mg/L, initial As(III) conc. = 0.5 mg/L; initial pH = 5.5, temp. = 22 ± 1 °C. MI: mono-ion, I: binary-ion.

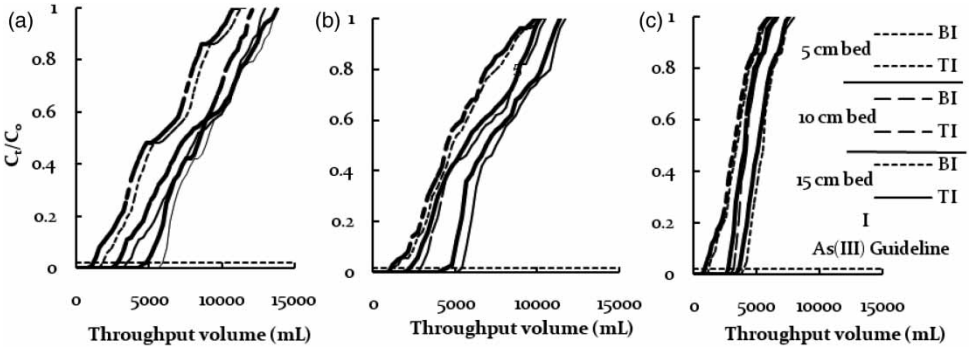

Figure 15 | Breakthrough trend of As(III) adsorption by PS bed depths of 5, 10 and 15 cm at flow rate of (a) 1.5 mL/min (b) 2.5 mL/min and (c) 3.5 mL/min from binary- and ternary-metal ion systems. Initial Fe(II) conc. = 5 mg/L, initial F^- conc. = 2 mg/L, initial As(III) conc. = 0.5 mg/L; initial pH = 5.5, temp. = 22 ± 1 °C. MI: mono-ion, I: binary-ion.

Table 13 | Summary of breakthrough throughput volumes and amount of ions adsorbed by PS beds from ternary-ion system comprised of Fe(II), F^- and As(III)

		Fe(II)		F^-		As(III)	
Flow rate (mL/min)	Bed depth (cm)	V_B (mL)	Amount adsorbed (mg)	V_B (mL)	Amount adsorbed (mg)	V_B (mL)	Amount adsorbed (mg)
1.5	5	1,890	8.88	1,350	1.35	1,200	0.588
	10	3,950	18.56	2,520	2.52	2,800	1.372
	15	5,940	27.91	4,100	4.10	4,860	2.381
2.5	5	1,250	5.87	1,080	1.08	1,100	0.539
	10	2,790	13.11	2,140	2.14	2,200	1.078
	15	5,450	25.61	3,300	3.30	4,550	2.229
3.5	5	1,120	5.26	1,100	1.10	900	0.441
	10	2,600	12.22	2,000	2.00	2,730	1.337
	15	4,400	20.68	3,150	3.15	3,570	1.749

metal ion which yielded critical breakthrough throughput from the ternary-ion system. The BDST parameters (N_o and K) were estimated for the adsorption of F^- from the ternary-ion system and are presented in Table 15.

The experimental BDST curves for F^- adsorption from the ternary-ion system were developed by plotting service times obtained at the critical breakthrough points with the respective bed depths (Figure 16). From

Table 14 | Ion adsorbed by PS beds from ternary-ion system comprised of Fe(II), F⁻ and As(III) up to critical breakthrough points with respect to F⁻

Flow rate (mL/min)	Bed depth (cm)	V_{BC} (mL)	Ion adsorbed Fe(II) (mg)	F⁻ (mg)	As(III) (mg)
1.5	5	1,350	6.51	0.65	1.350
	10	2,520	12.60	1.26	2.520
	15	4,100	20.50	2.05	4.100
2.5	5	1,080	5.12	0.53	1.080
	10	2,140	10.70	1.06	2.140
	15	3,300	16.50	1.65	3.300
3.5	5	1,100	5.30	0.52	1.100
	10	2,100	10.50	1.05	2.100
	15	3,150	15.75	1.58	3.150

V_{BC} = Critical breakthrough throughput volumes at effluent F⁻ ion conc. equal to regulatory limits.

Table 15 | Estimated BDST parameters for F⁻ adsorption from ternary-ion system comprised of Fe(II), F⁻ and As(III)

Ion (Initial conc.)	Flow rate (mL/min)	N_o (kg/m³)	K (m³/kg-min)	R^2
Fe(II) (5 mg/L) + F⁻ (2 mg/L) + As(III) (0.5 mg/L)	1.5	0.0780	1.612	0.9926
	2.5	0.0320	2.213	0.9975
	3.5	0.0188	5.267	0.9998

the experimental BDST curve obtained for a particular flow rate through the bed, efforts were made to model BDST curves for other two flow rates using Equations (5) and (6) and the modeled BDST curves were termed predicted BDST curves. For example, the experimental BDST curve obtained for F⁻ adsorption at a flow rate of 1.5 mL/min by PS beds from the ternary-ion system were used to develop the predicted BDST curves for the other two flow rates (Figure 16). Similar modeling was also carried out for F⁻ adsorption from the ternary-ion system by selecting the experimental BDST curve of another flow rate and predicting BDST curves for the remaining two flow rates. Errors involved in predicted and experimental BDST curves obtained for the other two flow rates while using the experimental BDST curve of a particular flow rate were estimated and shown in Table 16. The minimum and maximum errors involved between the predicted and experimental BDST curves varied between 3.97 and 26.12%.

CONCLUSION

1. A decrease in breakthrough throughput volumes were observed with increase in flow rates and decrease in bed depths, indicating decreased amount of Fe(II) and As(III) adsorbed by PS beds with increase in linear flow rates from mono- and binary-ion system comprised of Fe(II) and As(III).
2. The order of breakthrough of ions observed was As(III) followed by Fe(II), and F⁻ followed by Fe(II) in the binary-ion system of Fe(II) + As(III) and Fe(II)+ F⁻, and hence the breakthrough throughput volumes for As(III) in case of (Fe(II) + As(III)) and F⁻ in case of (Fe(II) + F⁻) is termed the critical breakthrough throughput volumes as Fe(II) is yet to breakthrough through the beds.
3. For the ternary-ion system comprised of Fe(II) + As(III) + F⁻, the order of breakthrough of ions was F⁻ followed by

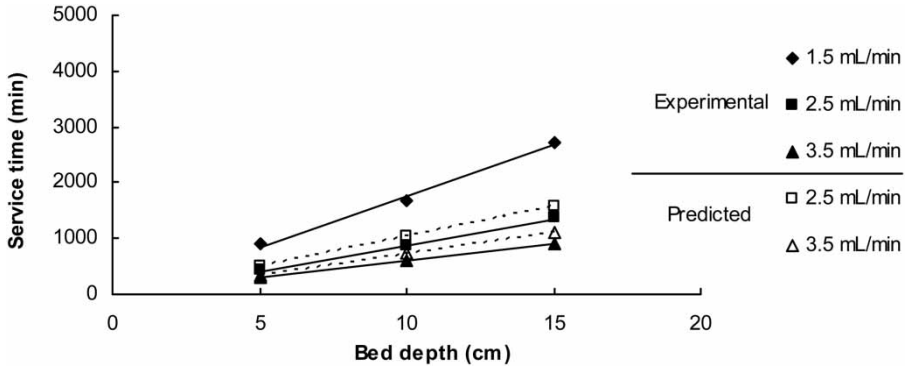

Figure 16 | Experimental and predicted BDST curves for F⁻ adsorption by PS beds at flow rates of 2.5 and 3.5 mL/min from ternary-metal ion system comprised of Fe(II), F⁻ and As(III). Experimental BDST curve at flow rate of 1.5 mL/min with initial Fe(II) conc. = 5 mg/L, initial F⁻ conc. = 2 mg/L and initial As(III) conc. = 0.5 mg/L used for prediction.

Table 16 | Estimated errors involved between predicted and experimental BDST values for F^- adsorption from ternary-ion system comprised of Fe(II), F^- and As(III)

Ion (initial conc.)	Selected flow rate (mL/min)	Predicted flow rate (mL/min)	Error (%) involved in service times for bed depth		
			5 cm	10 cm	15 cm
Fe(II) (5 mg/L) + F^- (2 mg/L) + As(III) (0.5 mg/L)	1.5	2.5	13.12	21.12	20.18
		3.5	5.96	21.42	24.92
	2.5	1.5	18.75	10.12	16.62
		3.5	7.92	3.97	6.98
	3.5	1.5	26.12	19.87	25.72
		2.5	9.11	6.14	8.24

As(III) and then by Fe(II) and hence F^- is termed critical breakthrough throughput volume.

4. A left-ward shifting of breakthrough trend lines for Fe(II), F^- and As(III) from binary- and ternary-ion systems compared to respective mono-ion systems is observed for all flow rates and bed depths indicating impact on the uptake of the selected ion by the presence of the other ion(s) in the binary- and ternary-ion systems.
5. The groundwater of Assam contains more than one ion and therefore, application of design-parameters obtained from the ternary-ion system of adsorption appears to be more appropriate choice for the design of adsorption column (or filter).

REFERENCES

Ahamad, K. U. 2010 Batch and Column Adsorption Studies for Simultaneous Removal of Iron, Arsenic and Fluoride by Wooden Charcoal and Sand used as Filter Media in Indigenous Household Iron Filter Units of Rural and Semi-urban Assam (India). PhD Thesis, Department of Civil Engineering, Indian Institute of Technology, Guwahati, India.

Ahamad, K. U. & Jawed, M. 2007 Role of wooden charcoal in indigenous household iron filters used in Assam (India). *Asian J. Water Environ. Pollut.* **5**, 23–28.

Ahamad, K. U. & Jawed, M. 2010 Kinetics, equilibrium and breakthrough studies for Fe(II) removal by wooden charcoal: a low-cost adsorbent. *Desalination* **251**, 137–145.

Andersson, A. & Johansson, J. 2002 Iron Removal from Groundwater in Rakai District, Uganda. Masters Thesis, Department of Environmental Engineering, Division of Sanitary Engineering, Lulea University of Technology, Sweden.

APHA 1998 *Standard Methods for the Examination of Water and Wastewater* 20th edn, American Public Health Association, American Water Works Association, Water Environment Federation, Washington, DC, USA.

Aziz, H. A., Yusoff, M. S., Adlan, M. N., Adnan, N. H. & Alias, S. 2004 Physicochemical removal of iron from semiaerobic landfill leachate by limestone filter. *Waste Manage.* **24** (4), 353–358.

Berg, M., Luzi, S., Trang, P. T., Viet, P. H., Giger, W. & Stüben, D. 2006 Arsenic removal from groundwater by household sand filters: comparative field study, model calculations, and health benefits. *Environ. Sci. Technol.* **40**, 67–73.

Bohart, G. S. & Adams, E. Q. 1920 Behaviour of charcoal towards chlorine. *J. Chem. Soc.* **42**, 523–529.

Buamah, R. 2009 Adsorptive Removal of Manganese, Arsenic and Iron from Groundwater. PhD Thesis, Wageningen University and UNESCO-IHE Institute for Water Education, Delft, The Netherlands.

Chibi, C. 1995 Design and performance of a community level iron removal plant. *Waterlines* **10**, 9–10.

Costodes, V. C. T., Fauduet, H., Porte, C. & Ho, Y. S. 2005 Removal of lead (II) ions from synthetic and real effluents using immobilized *Pinus sylvestris* sawdust: adsorption on a fixed-bed column. *J. Hazard. Mater.* **123**, 135–144.

Dahi, E. 1996 Contact precipitation for defluoridation of water. *Proc. at 22nd Water Engineering Development Center Conference*, New Delhi, India, pp. 262–265.

Das, B., Talukdar, J., Sarma, S., Gohain, B., Dutta, R. K., Das, H. B. & Das, A. C. 2003 Fluoride and other inorganic constituents in groundwater of Guwahati, Assam, India. *Curr. Sci.* **85**, 657–661.

Dzung, N. V., Phong, H. H., Long, N. N., Quang, N. T. & Waldemar, P. 2004 Domestic defluoridation of water using locally produced activated alumina. *Proc. 4th International Workshop on Fluorosis Prevention and Defluoridation of Water*, Colombo, Sri Lanka, pp. 69–74.

Ellis, D., Bouchard, C. & Lantagne, G. 2000 Removal of iron and manganese from groundwater by oxidation and microfiltration. *Desalination* **130**, 255–264.

Garelick, H. & Jones, H. (eds) 2008 *Arsenic Pollution and Remediation: An International Perspective. Reviews in Environmental Contamination and Toxicology Vol 197*. Springer, NewYork.

Goel, J., Kadirvelu, K., Rajagopal, C. & Garg, V. K. 2005 Removal of lead(II) by adsorption using treated granular activated carbon: batch and column studies. *J. Hazard. Mater.* **125**, 211–220.

Hutchins, R. A. 1973 New method simplifies design of activated carbon systems. *Chem. Eng.* **80**, 133–138.

Ikuo, A., Satoshi, I., Toshimitsu, T., Naohito, K., Takeo, N. & Seiki, T. 2004 Adsorption of fluoride ions onto carbonaceous materials. *J. Colloid Interface Sci.* **275**, 35–39.

IS 10500 1991 *Specification for Drinking Water*. Bureau of Indian Standards, New Delhi.

IS 2720 1975 *Methods for Test for Soil Grain Size Analysis (Part IV)*. Bureau of Indian Standards, New Delhi.

Khan, A. H., Rasul, S. B., Munir, A. K. M., Alauddin, M., Habibuddowlah, M. & Hussam, A. 2000 *On Two Simple Arsenic Removal Methods for Groundwater of Bangladesh*. http://www.eng-consult.com/arsenic/Tech-hussam.PDF (accessed 19 February 2013).

Larsen, M. J. & Pearce, E. I. F. 1992 Partial defluoridation of drinking water using fluorapatite precipitation. *Caries Res.* **26**, 22–28.

Lehman, M., Zouboulis, A. I. & Matis, K. A. 2001 Modelling the sorption of metals from aqueous solutions on goethite fixed-beds. *Environ. Pollut.* **113**, 121–128.

Mahanta, D. B., Das, N. N. & Dutta, R. K. 2004 A chemical and bacteriological study of drinking water in tea gardens of central Assam. *Ind. J. Environ. Proc.* **24**, 654–660.

Meenakshi, S. & Maheshwari, R. C. 2006 Fluoride in drinking water and its removal. *J. Hazard. Mater.* **137**, 456–463.

Munter, R., Ojaste, H. & Sutt, J. 2005 Complexed iron removal from groundwater. *J. Environ. Eng.* **131**, 1014–1020.

Muraleedharan, T. R., Ligy, P. & Iyenger, L. 1994 Application studies of biosorption for monazite processing industry effluents. *Bioresour. Technol.* **49**, 179–186.

Ngai, T. K., Shrestha, R. R., Dangol, B., Maharjan, M. & Murcott, S. E. 2007 Design for sustainable development – household drinking water filter for arsenic and pathogen treatment in Nepal. *J. Environ. Sci. Health A Tox./Hazard. Subst. Environ. Eng.* **42**, 1879–1888.

Othman, M. Z., Roddick, F. A. & Snow, R. 2001 Removal of dissolved organic compounds in fixed-bed columns: evaluation of low-rank coal adsorbents. *Water Res.* **35**, 2943–2949.

Petrusevski, B., Sharma, S., Vander-Meer, W. G., Kruis, F., Khan, M., Barua, M. & Schippers, J. C. 2008 Four years of development and field-testing of IHE arsenic removal family filter in rural Bangladesh. *Water Sci. Technol.* **58**, 53–58.

Rajchagool, S. & Rajchagool, C. 1997 Solving the fluorosis problem in a developing country. *Proc. 2nd International Workshop on Fluorosis and Defluoridation of Water*, Addis Ababa, Ethiopia.

Rao, G. V. R. S. & Rekha, D. S. 2004 A study of the removal of dissolved iron from ground water using bio-filtration technique. *Indian J. Public Health* **1**, 29–31.

Sarkar, A., Choudhury, U. K., Rahman, M. H. & Choudhury, T. R. 2000 Bucket treatment unit for arsenic removal, Water, Sanitation and Hygiene: Challenges of the Millennium. *Preprints of 26 Water Engineering Development Center Conference*, Dhaka, Bangladesh, pp. 308–310.

Sharma, R., Shah, S. & Mahanta, C. 2005 Hydrogeochemical study of groundwater fluoride contamination: a case study from Guwahati city, India. *Asian J. Water Environ. Pollut.* **2**, 47–54.

Singh, A. K. 2004 Arsenic contamination in groundwater of North Eastern India. *Proc. of National Seminar on Hydrology with Local Theme on Water Quality, National Institute of Hydrology*, Roorkee, India. www.physics.harvard.edu/~wilson/arsenic/references/singh.pdf (accessed 19 February 2012).

Sudipta, S., Anirban, G., Ranjan, K. B., Arun, K. D., John, E. G. & Arup, K. S. 2005 Well-head arsenic removal units in remote villages of Indian subcontinent: field results and performance evaluation. *Water Res.* **39**, 2196–2206.

Vaaramaa, K. & Lehto, J. 2003 Removal of metals and anions from drinking water by ion exchange. *Desalination* **155**, 157–170.

Venkobachar, C., Iyengar, L. & Mudgal, A. K. 1997 Household defluoridation of drinking water using activated alumina. *Proc. of 2nd International Workshop on Fluorosis Prevention and Defluoridation of Water*, Nazreth, Ethiopia, pp. 138–145.

WHO 1993 *Guidelines for Drinking Water Quality, 2nd Edition, Vol. I Health Criteria and Supporting Information, Recommendations*. World Health Organization, Geneva, Switzerland.

First received 19 July 2012; accepted in revised form 14 January 2013. Available online 7 March 2013